Jun Meng[1], Yue Huang[1*], Danny M. Leung[1], Longlei Li[2], Adeyemi A. Adebiyi[1,†], Claire L. Ryder[3], Natalie M. Mahowald[2], Jasper F. Kok[1]

[1]Department of Atmospheric and Oceanic Sciences, University of California, Los Angeles, CA 90095, USA

[2]Department of Earth and Atmospheric Sciences, Cornell University, Ithaca, NY 14850, USA

[3]Department of Meteorology, University of Reading, RG6 6BB, Reading UK

Corresponding author: Jun Meng (jun.meng@ucla.edu)

†Additional author notes should be indicated with symbols (current addresses, for example).

*Now at Earth Institute, Columbia University, New York, NY 10025, USA and NASA Goddard Institute for Space Studies, New York, NY 10025, USA

†Now at Department of Life & Environmental Sciences, University of California, Merced, CA 95343, USA

Key Points:

- We develop a model parameterization for the size distribution of emitted dust aerosols that includes emission of super coarse dust
- The parameterization enables models to reproduce measurements of super coarse atmospheric dust near dust source regions
- The remaining underestimation of super coarse dust over dust outflow regions is likely due to errors in models' deposition processes

Abstract

Aircraft measurement campaigns have revealed that super coarse dust (diameter > 10 m) surprisingly accounts for approximately a quarter of aerosols by mass in the atmosphere. However, most global aerosol models either underestimate or do not include super coarse dust abundance. To address this problem, we use brittle fragmentation theory to develop a parameterization for the emitted dust size distribution that includes emission of super coarse dust. We implement this parameterization in the Community Earth System Model (CESM) and find that it brings the model in good agreement with measurements of super coarse dust close to dust source regions. However, the model still underestimates super coarse dust in dust outflow regions. Thus, we conclude that model underestimation of super coarse atmospheric dust is in part due to the underestimation of super coarse dust emission and likely in part due to errors in deposition processes.

Plain Language Summary

Aircraft measurements have found surprisingly large concentrations of super coarse atmospheric dust (diameter > 10 m), which accounts for approximately a quarter of particulate matter mass in the atmosphere. However, current atmospheric models do not include or cannot reproduce this abundance of super coarse dust. Here we develop a parameterization for the emission of super coarse dust. We evaluate this new parameterization in the Community Earth System Model (CESM) and find that it enables the model to reproduce in situ aircraft measurements of super coarse atmospheric dust near dust source regions. However, the model still underestimates super coarse atmospheric dust over dust outflow regions, possibly due to errors in deposition processes. We further find that the equivalent effect of possible errors in dust deposition processes during transport is to decrease the effective dust aerosol density in the model to an order of magnitude of its physical value of ~2500 kg/m^3. Thus, we conclude that the underestimation of super coarse atmospheric dust by models is in part due to the underestimation of the emission of super coarse dust and likely in part due to errors in deposition processes.

1 Introduction

Mineral dust is an important component of the Earth system, impacting radiation, clouds, biogeochemistry, and air quality (Chen et al., 2019; Guieu et al., 2019; Jickells et al., 2005; Kosmopoulos et al., 2017; Meng et al., 2021). Because all these impacts depend sensitively on dust size (Mahowald et al., 2014), global aerosol models need to accurately represent the dust particle size distribution (PSD) to quantify the various dust impacts on the Earth system. Recent airborne dust PSD measurements from several field campaigns have shown that super coarse (diameter > 10 m) dust particles are more prevalent than previously thought (van der Does et al., 2018; Ryder et al., 2018, 2019; Varga et al., 2021). Indeed, recent estimates suggest an atmospheric load of ~10 Tg of super coarse dust, which represents about a quarter of the total atmospheric loading of particulate matter (Adebiyi & Kok, 2020; Di Biagio et al., 2020; Kok et al., 2021). However, some current models do not include super coarse dust (Kok, Albani, et al., 2014; Wu et al., 2020; Zhang et al., 2013). Other models that do represent super coarse dust underestimate their abundance by over an order of magnitude (Adebiyi and Kok, 2020). This omission or underestimation of super coarse dust by models hinder our quantitative understanding of how dust aerosols affect the current and future climates (Kok et al., 2017; Ryder et al., 2019; Adebiyi and Kok, 2020).

To enable models to account for more accurate abundance of airborne super coarse dust, we develop a new parameterization of the PSD of emitted dust that accounts for the emission of super coarse dust (Section 2). We implement this new parameterization in the Community Earth System Model (CESM, version 1.2) and evaluate the simulated atmospheric dust PSD with in situ aircraft measurements (Section 3&4). We find that the model with this new parameterization reproduces the abundance of super coarse dust close to dust source regions. We also discuss possible reasons why the model still underestimates

super coarse dust further from source regions (Section 5).

2 Derivation of parameterization of emitted dust size distribution including super coarse dust

In this section, we first review the original brittle fragmentation theory for parameterizing the emitted dust size distribution (Section 2.1). We then extend it to account for super coarse dust emission (Section 2.2).

2.1 Original brittle fragmentation theory

The emitted dust PSD depends on the physical process of dust emission. Instead of being lifted directly by wind, dust aerosols are therefore usually emitted from the energetic impacts of bouncing or saltating larger sand-sized particles (~70 - 500 m) onto dust aggregates in the soil, a process known as sandblasting (Kok, Mahowald, et al., 2014; Shao, 2008). When a saltating particle strikes a soil dust aggregate, the impact creates elastic waves that can rupture the interparticle bonds between particles in the dust aggregate. Since dry dust aggregates are usually brittle (Braunack et al., 1979; Perfect & Kay, 1995), Kok (2011a) hypothesized that dry soil dust aggregates shatter upon impact by an energetic saltating particle in much the same way that brittle materials, such as glass, shatter upon a sufficiently energetic impact. This hypothesis is supported by the observation that measurements of the emitted dust size distribution follow the power law observed for brittle fragmentation in the 1-10 m diameter range (Supplementary Figure S1).

By assuming that most dust aerosol emissions are the result of fragmentation of dry soil dust aggregates by impacting saltators, Kok (2011a) proposed an expression for the size distribution of emitted dust aerosols with diameter smaller than 20 m:

$$\frac{dV_{\text{emis}}}{\text{dlnD}} = \frac{D}{c_v}\left[1+\text{erf}\left(\frac{\ln\left(D/\overline{D_s}\right)}{\sqrt{2}\ln\sigma_s}\right)\right]\exp\left[-\left(\frac{D}{\lambda}\right)^3\right], \quad (1)$$

where V_{emis} is the normalized volume of dust aerosol with geometric diameter D, c_v is a normalization constant ensuring that the integral over $\frac{dV_{\text{emis}}}{\text{dlnD}}$ equals 1, and $\overline{D_s}$ and σ_s are the median diameter and geometric standard deviation of the log-normal distribution of the fully dispersed soil size distribution. The parameter λ is the side crack propagation length, which denotes the propagation distance of side branches of cracks created in the soil dust aggregate by a fragmenting impact. Experimental data indicate that λ is of the order of 10% of the size of the object being fragmented (Herrmann & Roux, 2014; Oddershede et al., 1993). Based on a fit to the available data at that time, Kok (2011a) used $\lambda = 12$ m, thereby implicitly assuming that the fragmentation of all soil dust aggregates are governed by a similar side crack propagation length, even though soil dust aggregates can differ notably in size (e.g. Chatenet et al., 1996; Klose et al., 2017).

This brittle fragmentation theory (hereafter BFT-original) (Eq. 1) is in good agreement with measurements of the emitted dust size distribution for dust par-

ticles smaller than 10 m in diameter (Kok, 2011a; Rosenberg et al., 2014; Shao et al., 2011), including several data sets published after the publication of BFT-original (Figure 1a). Therefore, it has been extensively used in global aerosol models (e.g., Zhang et al., 2013; Albani et al., 2014; Ito et al., 2012). However, recent work has indicated that BFT-original substantially underestimates the emission of super coarse dust (diameter > 10 m) (Rosenberg et al., 2014; Huang et al., 2021). The emission in that size range is largely determined by the value of the side crack propagation length (λ).

2.2 Extending brittle fragmentation theory to account for super coarse dust emission

We develop a parameterization that accounts for super coarse dust emission (hereafter BFT-coarse). We do so by extending brittle fragmentation theory (Eq. 1) to include a more realistic description of the size-crack propagation length (λ), which determines the cut-off diameter above which aerosols are no longer created through fragmentation. Since λ scales with the size of the object (e.g. soil dust aggregate) being fragmented (Herrmann & Roux, 2014; Oddershede et al., 1993), it will be a function of the size of the soil dust aggregate being fragmented. That is,

$$= f_\lambda D_{\mathrm{agg}}, \quad (2)$$

where $f_\lambda \sim 0.1$ is the ratio of to the dust aggregate size (Herrmann & Roux, 2014; Oddershede et al., 1993) and D_{agg} is the diameter of the fragmented soil dust aggregate. We account for the dependence of λ on the soil aggregate diameter by substituting Eq. (2) into Eq. (1), accounting for the probability distribution $P_{\mathrm{agg}}(D_{\mathrm{agg}})$ of the diameter of soil aggregates, and then integrating over the size of soil dust aggregates that can be fragmented to produce dust aerosols:

$$\frac{dV_{\mathrm{emis}}}{\mathrm{dlnD}} = \frac{D}{c_v}\left[1+\mathrm{erf}\left(\frac{\ln(D/\overline{D_s})}{\sqrt{2}\ln\sigma_s}\right)\right]\int_0^\infty \exp\left(-\frac{D}{f_\lambda D_{\mathrm{agg}}}\right)^3 P_{\mathrm{agg}}(D_{\mathrm{agg}})dD_{\mathrm{agg}}, \quad (3)$$

where V_{emis} is the normalized volume of dust aerosol with size D, c_v is a normalization constant ensuring that the integral of $\frac{dV_{\mathrm{emis}}}{\mathrm{dlnD}}$ equals 1 over the size range 0.1 to 20 m (following Kok, 2011a), and $\overline{D_s} = 1.13 \pm 0.58$ and $\sigma_s = 1.92 \pm 0.25$ were obtained by optimizing agreement against measurements, as detailed in Kok et al. (2017) and Huang et al. (2021).

The available measurements indicate that the size distribution of minimally dispersed soil particles in arid soils generally follows a lognormal distribution (Butler et al., 2013; Chatenet et al., 1996; Klose et al., 2017). Assuming that the size distribution of fragmented soil dust aggregates (P_{agg}) bears a close resemblance to the size distribution of undisturbed soil particles, we can write $P_{\mathrm{agg}}(D_{\mathrm{agg}})$ as:

$$P_{\mathrm{agg}}\left(D_{\mathrm{agg}}\right) = \left(\frac{1}{D_{\mathrm{agg}}\sigma_{\mathrm{agg}}\sqrt{2\pi}}\right)\exp\left(-\frac{\left(\ln\left(D_{\mathrm{agg}}\right) - \ln\left(\overline{D_{\mathrm{agg}}}\right)\right)^2}{2{\sigma_{\mathrm{agg}}}^2}\right), \quad (4)$$

where σ_{agg} and $\overline{D_{\mathrm{agg}}}$ are the geometric standard deviation and median diameter of the log-normal distribution of the minimally dispersed soil size distribution. We obtain the parameters (σ_{agg} and $\overline{D_{\mathrm{agg}}}$) of the soil dust aggregates size distribution $P_{\mathrm{agg}}(D_{\mathrm{agg}})$ in Eq. 4 by analyzing a compilation of measurements of the minimally dispersed size distribution in arid soils and fitting lognormal distributions to the measurements. A detailed description of the compilation of soil aggregate PSD measurements can be found in the supplement (SI. S1). The results indicate that the parameters of the soil dust aggregate size distribution are relatively constant and do not correlate with soil texture, which is consistent with previous work (Chatenet et al., 1996; Laurent et al., 2006). Therefore, these parameters can be described by a constant median diameter ($\overline{D_{\mathrm{agg}}}$) of 127 $\pm$ 47 m and geometric standard deviation (σ_{agg}) of 2.95 $\pm$ 1.01 for the soil dust aggregate size distribution. We calculate the error bounds (uncertainty) on the theoretical prediction by using a bootstrap method combined with a maximum likelihood method that propagates errors in $\overline{D_s}$, σ_s, $\overline{D_{\mathrm{agg}}}$, and σ_{agg}, following the approach in Kok et al. (2017).

The new BFT-coarse parameterization derived here is in good agreement with the limited measurements of the emission of super coarse dust (Fig. 1a). However, there are few measurements of the emitted dust PSD that extend to the super coarse dust size range because such large particles are usually lost in instrument inlets due to their high inertia (Rosenberg et al., 2014; von der Weiden et al., 2009). In order to better determine whether the new emitted dust PSD parameterization reasonably represents the emission of super coarse dust, in the next section we use global aerosol model simulations to further evaluate the parameterization against aircraft measurements of freshly emitted atmospheric dust. These aircraft measurements were acquired by wing-mounted probes and did not suffer from inlets restricting measurements of coarse particles (Ryder et al., 2015, 2018).

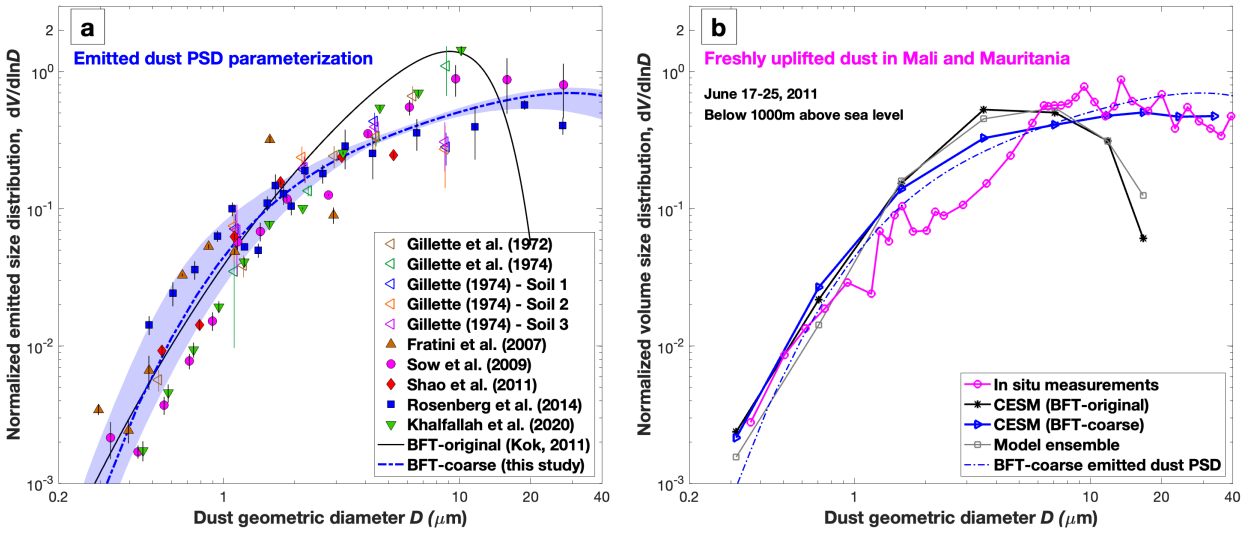

Figure 1. The parameterization for the emission of super coarse dust reproduces measurements of emitted and freshly lifted super coarse dust. Shown are (a) comparison between the parameterization and measurements of the normalized PSD of emitted dust and (b) comparison of the simulated and measured atmospheric PSD of freshly uplifted dust. In (a), different markers denote observations of the emitted dust PSD from different studies, which were described and corrected to geometric diameter as detailed in Huang et al. (2021). Vertical error bars denote the standard error of measurements under various wind events at a given soil (see Kok et al., 2017), the black line denotes the dust PSD predicted by the original brittle fragmentation theory (BFT-original), and the blue dash-dotted line denotes the parameterization of emitted dust developed in this study (BFT-coarse). Blue shading denotes the 95% confidence interval. In (b), the magenta open circles denote the average PSD of freshly uplifted dust over Mali and Maritania (~23.5°N, 7°W) during FENNEC campaign (flights B600, B601, B602 and B610 at altitudes below 1000 m). The black and blue lines with different markers show the simulated atmospheric dust PSD with the original emitted dust PSD (BFT-original) and the new emitted dust PSD parameterization (BFT-coarse; the blue dash-dotted line), respectively. The gray line denotes the seasonally averaged (JJA) dust PSD from an ensemble of global model simulations (Adebiyi et al., 2020). Locations of the measurements are shown in Figure S2. All curves are normalized to yield unity when integrated over the 0.1-20 m diameter range.

3 Methodology for evaluating super coarse dust emission parameterization against in situ measurements using CESM simulations

3.1 Aircraft measurements of atmospheric dust PSD

We compiled atmospheric dust PSD measurements from several aircraft measurement campaigns near dust source regions and over dust outflow regions.

We used measurements of freshly uplifted dust and aged dust near dust source regions from the FENNEC 2011 aircraft campaign over western North Africa (Ryder et al., 2015). Specifically, we used measurements of (i) freshly uplifted dust (FENNEC flights B600, B601, B602 and B610), (ii) advected aged dust emitted from the Atlas Mountains (flights B605 and B606), and (iii) advected aged dust emitted from Mauritania (flights B609, B611, B612, and B613). The source regions for dust sampled during each flight were determined using back-trajectory analysis (Ryder et al., 2015). All the three categories of measurements assumed dust particles to be spherical, and we corrected them to account for dust asphericity following Huang et al. (2021), which is critical because ignoring dust asphericity causes an overestimate of dust particle size at coarse sizes (Fig. S5). We then averaged over all measurements in each of the three categories.

In addition to the FENNEC, we used aircraft measurements of long-range transported dust over dust outflow regions, including from the Saharan Mineral Dust Experiment (DARPO) over southern Portugal (Wagner et al., 2009), from the FENNEC-SAL campaign over the Canary islands (Ryder, Highwood, Lai, et al., 2013), and from the Saharan Aerosol Long-Range Transport and Aerosol-Cloud-Interaction experiment (SALTRACE) over Barbados and Cape Verde (Weinzierl et al., 2017). Because exact specifications of the instrumentation used in these campaigns were not conveniently available, these measurements were not corrected for dust optical properties and asphericity (Huang et al., 2021).

A detailed description of all aircraft measurements used in this study is provided in the supplement (SI. S2).

3.2 CESM model, simulations and model emsemble

We used CESM version 1.2 (Hurrell et al., 2013) with the Community Atmosphere Model version 4.0 (CAM4) (Neale et al., 2010) as the atmosphere component. This version of the model uses externally mixed particle bins to simulate dust. We added four extra coarse bins (10-14, 14-20, 20-28, and 28-40 µm) in addition to the four default bins (0.1-1, 1-2.5, 2.5-5, and 5-10 µm). The dust emission module is a physically based dust emission parameterization derived in Kok, Mahowald, et al. (2014). The mass fraction of emitted dust in each model bin, which represents the emitted dust PSD in the model, is calculated from the original (BFT-original) and the new (BFT-coarse) dust emission PSD parameterization. Dust dry deposition in CESM accounts for gravitational settling and turbulent deposition processes (see Section 2.8 in Zender et al., 2003), which are dust size and density dependent. We accounted for the effect of dust asphericity dy decreasing the gravitational settling velocity by 13% following Huang et al. (2020). A detailed description of the CESM model is provided in the supplement (SI. S3).

We conducted CESM simulations nudged towards MERRA2 dynamics. We used a horizontal resolution of 1.9°x2.5° and 56 vertical levels and simulated the period 2006 – 2015, which overlaps with the years that available aircraft measurements were taken. For model comparisons against measurements of freshly

lifted dust events, we included dust emission only from the grid box from which the sampled dust was emitted, as determined from backwards trajectory analyses (Ryder et al., 2015). For model comparisons against other measurements, including aged dust and long range transported dust, we included dust emission for all grid boxes in the model. We also conducted a set of simulations with the new BFT-coarse PSD parameterization that use dust aerosol densities of 125 kg m^{-3}, 250 kg m^{-3}, 500 kg m^{-3}, and 1000 kg m^{-3}, which are substantially smaller than the physical density of 2500 kg m^{-3}. The objective of these simulations was to quantify the effect of the missing or erroneously-described processes that cause an apparent overestimation of the deposition and underestimation of the long-range transport of super coarse dust (Ansmann et al., 2017; Weinzierl et al., 2017). We averaged our model simulation during the daytime (10:00 -18:00 local time) for the days for which measurements were made. We also tested averaging our model simulation over different temporal resolutions and found that the simulated atmospheric dust PSDs shows limited sensitivity to the averaging period (Figure S3).

To evaluate the performance of current models in simulating super coarse dust, we also compare our simulated atmospheric dust PSD with the atmospheric dust PSD from an ensemble of model simulations. This model ensemble was obtained in Adebiyi et al. (2020) and used simulations from six different models that provide seasonally averaged atmospheric dust PSD (see Supplement).

4 Evaluation of super coarse dust emission parameterization against in situ measurements using CESM simulations

We first evaluate the simulations against in situ aircraft measurements taken close to dust source regions, which shows a significant improvement of the new emitted dust PSD parameterization in reproducing the super coarse atmospheric dust over dust source regions (Section 4.1). Subsequently, we evaluate the simulated dust PSD against measurements taken in dust outflow regions, finding that CESM still underestimates long-range transported super coarse atmospheric dust (Section 4.2).

4.1 Comparison against measurements near dust source regions

Measurements of the atmospheric dust size distribution over dust source regions are well suited to evaluate the accuracy of the super coarse dust PSD parameterization because these measurements are minimally affected by dust transport and deposition, which models struggle to simulate accurately (Adebiyi & Kok, 2020; Di Biagio et al., 2020). We thus compare the atmospheric dust PSD from the simulations with the BFT-original and BFT-coarse emitted dust PSDs against in situ measurements of the PSD of freshly uplifted dust in western North Africa from the FENNEC 2011 campaign (Figure 1b). As expected, the simulated freshly uplifted atmospheric dust PSD is highly similar to the parameterized emitted dust PSD. We find that the simulation with the new BFT-coarse dust emission PSD parameterization reproduces the measurements of the PSD of freshly lifted atmospheric dust over the dust source

region, notably including the super coarse dust size range. In contrast, both the model ensemble and the CESM simulation with the BFT-original parameterization substantially underestimate the abundance of super coarse atmospheric dust. This result indicates that the new dust emission PSD parameterization can reasonably represent the emission of super coarse dust.

Next, we evaluate the model performance with BFT-coarse against aged atmospheric dust PSD measurements taken close to dust source regions. These measurements sampled atmospheric dust that was not locally emitted but rather was aged and transported from nearby dust source regions (Ryder et al., 2015). Figure 2 shows the atmospheric dust PSD simulated using both the BFT-original and the BFT-coarse emitted dust PSDs, as well as the PSD from the model ensemble. We find that the simulation with the new BFT-coarse parameterization is consistent with measurements of the PSD of aged dust close to the surface (Figs. 2a & 2b), with super coarse dust with $D > 20$ m becoming somewhat underestimated with increasing altitude (Figs. 2c - d). In contrast, the model ensemble and the simulation with the BFT-original emitted dust PSD substantially underestimates super coarse dust at all altitudes.

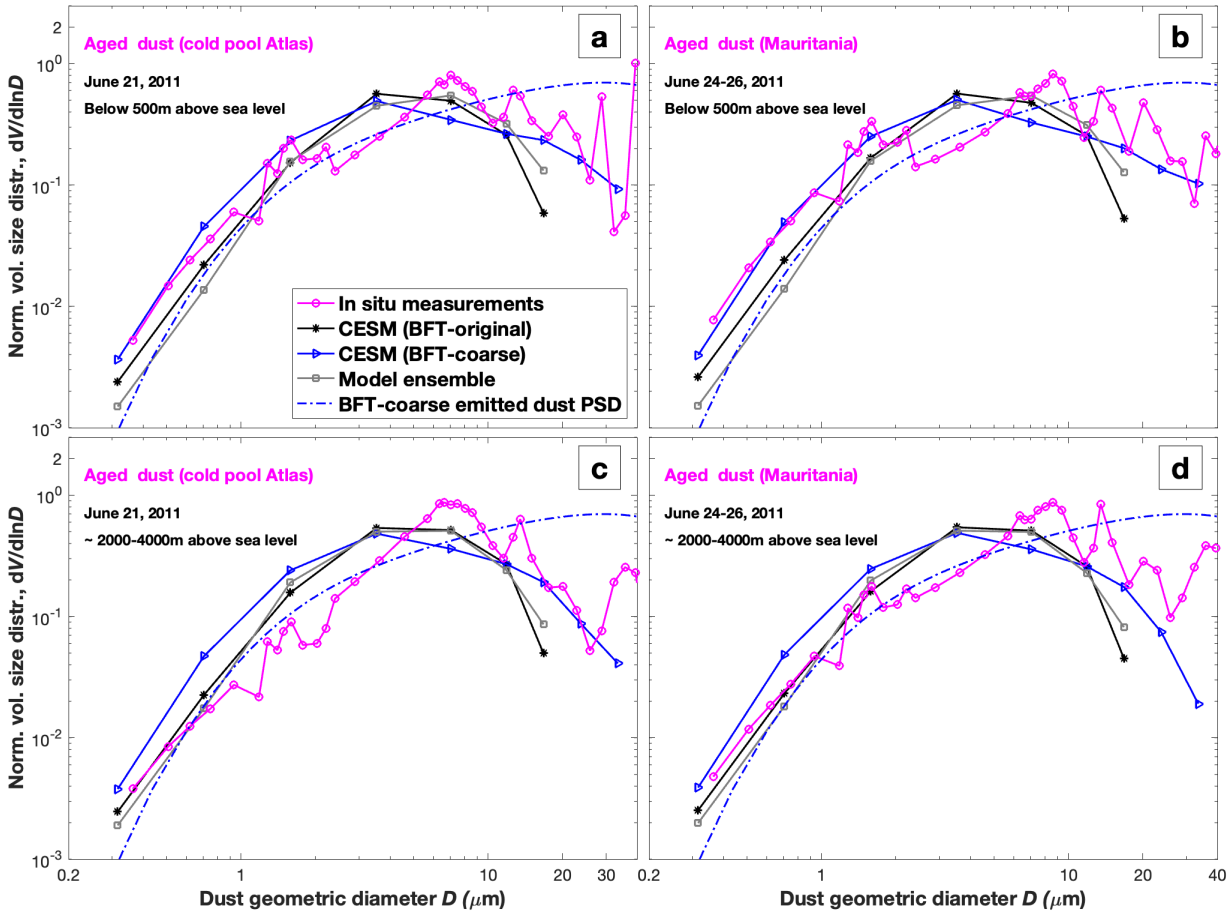

Figure 2. Comparison between simulations and measurements of the PSD of aged dust near source regions. Shown are CESM simulations using both the upgraded BFT-coarse (blue line with triangle markers) and the original BFT-original dust emission PSD (black line with asterisk markers), as well as the seasonally averaged dust PSD (grey line with square markers) from an ensemble of model simulations (Adebiyi et al., 2020). The blue dash-dotted line denotes the parameterization of emitted dust developed in this study (BFT-coarse). Atmospheric dust PSD measurements (magenta open circles) are from FENNEC 2011 flights that measured aged dust events, including aged dust from a cold pool near the Atlas mountains (flights B605 and B606) and from Mauritania (flights B609, B611-613) (Ryder et al., 2015). Locations of the measurements are shown in Figure S2. All curves are normalized to yield unity when integrated over the 0.1-20 m diameter range.

4.2 Underestimation of super coarse atmospheric dust over dust outflow regions

To examine whether our new parameterization enables models to also effectively

represent super coarse dust further away from dust source regions, we compare the simulated atmospheric dust PSD against measurements taken in dust outflow regions. We find that, despite the significant improvement produced by BFT-coarse in representing super coarse dust near dust source regions (Figure 1b & 2), our CESM simulation with BFT-coarse still underestimates super coarse dust in dust outflow regions, such as the eastern Atlantic Ocean and the Caribbean region (Figure 3). Moreover, the magnitude of the underestimation becomes larger as the distance of the measurement location from dust source regions increases. For example, the underestimation of super coarse dust with $D > 20$ µm over Barbados (Figure 3f) is substantially larger than that over Cape Verde (Figure 3e). This suggests that the underestimation is due to errors in the model's dust deposition processes or vertical numerical diffusion during dust transport.

In order to quantify model errors due to the underestimation of the super coarse dust lifetime, we test whether a decreased dust aerosol density yields a more realistic abundance of super coarse dust further from source regions. Indeed, our sensitivity simulations using smaller dust aerosol densities show greatly improved agreement with observations over the desert outflow regions (Fig. 3). Optimal agreement is produced with simulations using 125 kg/m3 and 250 kg/m3, for which the lifetime of super coarse dust is increased by over an order of magnitude (Fig. S6). This suggests that the equivalent effect of possible errors in dust deposition processes during dust transport is to underestimate the lifetime of super coarse dust by an order of magnitude. Although it would be preferable to address the model errors that cause the underestimation of super coarse dust lifetime, our results suggest that decreasing the modeled dust aerosol density by 10 to 20 times its physical value of ~2500 kg/m3 could be useful in more accurately simulating the long-range transport of super coarse dust.

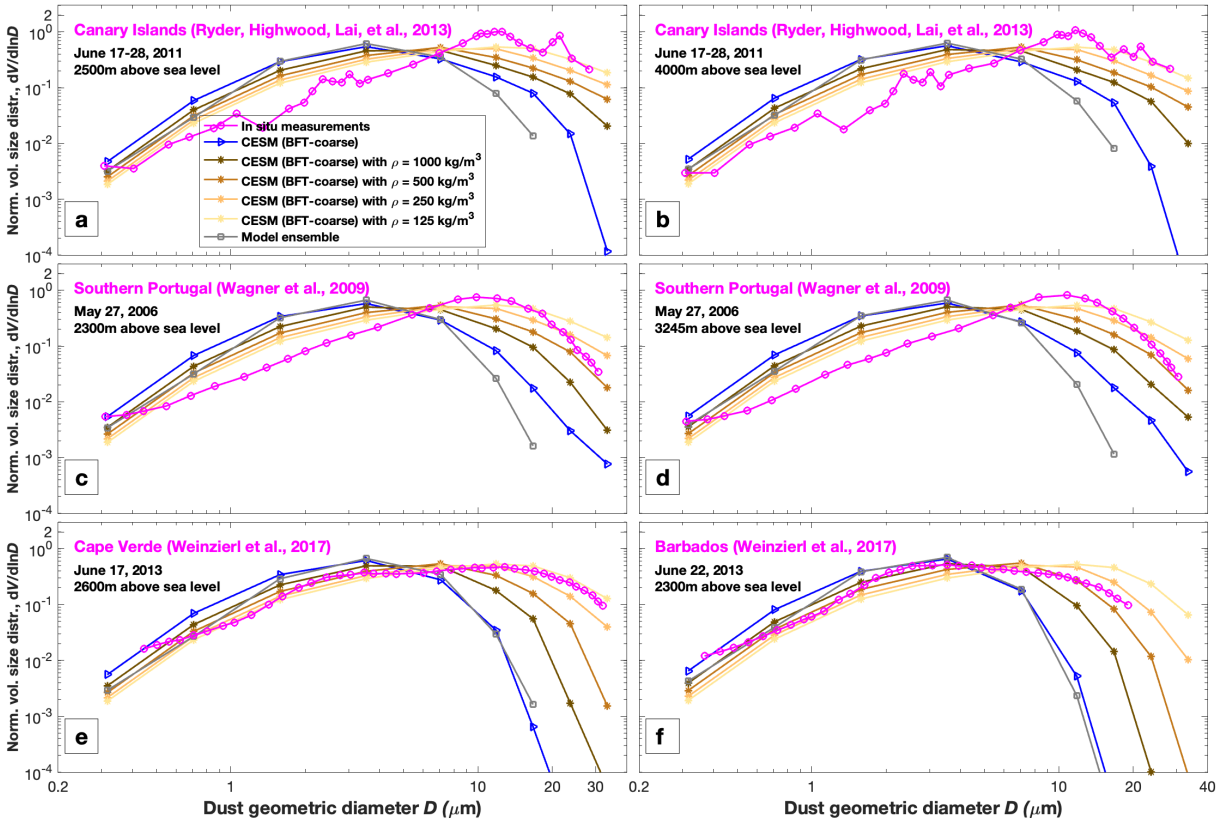

Figure 3. Comparison between simulations and measurements of the dust PSD in dust outflow regions. Simulated atmospheric dust PSDs include a simulation using the default dust aerosol density (2500 kg m^{-3}, blue line with triangle markers) and four simulations using smaller dust aerosol densities (1000 kg m^{-3}, dark brown line; 500 kg m^{-3}, brown line; 250 kg m^{-3}, orange line; 125 kg m^{-3}, light yellow line); all simulations use the BFT-coarse emitted dust PSD. The gray line is the seasonally averaged dust PSD from an ensemble of model simulations (Adebiyi et al., 2020). Measurements (magenta open circles) include the dust PSD over the Canary Islands (~28°N, 16°W) at two altitudes (2500m and 4000m) (Ryder, Highwood, Lai, et al., 2013), over southern Portugal (~38°N, 8°W) at two altitudes (2300m and 3245m) (Wagner et al., 2009), and at Cape Verde (~15°N, 23°W) and Barbados (~12°N, 60°W) (Weinzierl et al., 2017). Locations of the measurements are shown in Figure S2. All curves are normalized to yield unity when integrated over the 0.1-20 m diameter range.

5 Discussion and Perspectives

We have presented a new parameterization for the emitted dust PSD that accounts for the emission of super coarse dust (Figure 1a). Our evaluation of this new parameterization using CESM has shown that it can reproduce the

abundance of super coarse dust close to dust source regions (Figures 1b & 2). However, we also find that CESM still greatly underestimates super coarse dust far from source regions (Figure 3).

These findings imply that errors in model processes besides emission, most likely in dust deposition and numerical diffusion, contribute to the underestimation of super coarse dust in models, as previously hypothesized (van der Does et al., 2018; Adebiyi and Kok, 2020). Such possible model errors include, first, an overestimation of the gravitational setting speed of (super) coarse dust. This could be because vertical electric fields generated by charged dust particles in the atmosphere might generate electric forces that counter gravitational settling (Renard et al., 2018; Ulanowski et al., 2007), or because turbulence in dusty air layers counteracts gravitational settling (Gasteiger et al., 2017). Second, the vertical transport of (super) coarse dust might be underestimated. In particular, a recent study has shown that topography greatly enhances the upward vertical transport of super coarse dust in the boundary layer (Heisel et al., 2021). This effect is not fully accounted for in most models and could help explain the remaining slight underestimation of super coarse dust near source regions (Fig. 1b and 2). Additionally, the current available meteorological wind field that drives the model might not capture convection events that lift super coarse dust higher into the boundary layer (Cowie et al., 2015; Roberts et al., 2017). Third, although the Piecewise Parabolic Method transport scheme used in CAM4 produces relatively little numerical diffusion (Neale et al., 2010), it is nonetheless possible that numerical diffusion in CAM4 causes an overestimate of dust deposition (Ginoux, 2003; Rastigejev et al., 2010). Therefore, improvements in dry deposition schemes, meteorological input fields, and advective transport schemes might be needed to correctly simulate the long-range transport of (super) coarse dust. However, until that is achieved, our findings indicate that reducing the dust aerosol density in the model by 10 to 20 times can serve as a proxy for these missing or erroneously parameterized processes.

This work has a few limitations. First, the emission of super coarse dust depends on the size distribution of soil aggregates, which is uncertain (e.g., Shao, 2011; Klose et al., 2017). Second, the derived updated emitted dust PSD inherently assumes that fragmentation of soil aggregates dominates the dust emission process (Kok, 2011a). As such, we do not account for the effect of other emission processes, such as removal of clay coatings, aerodynamic entrainment, and direct emission of soil particles, all of which might dominate for certain soils and environmental conditions (Huang et al., 2019; Klose & Shao, 2012). Moreover, we do not account for a possible dependence of the emitted dust PSD on wind speed (Kok, 2011b; Shao et al., 2020).

6 Conclusions

We have extended the brittle fragmentation theory for the emitted dust particle size distribution in order to account for the emission of super coarse dust. This new parameterization could improve current global aerosol models, which generally neglect or greatly underestimate super coarse dust (Adebiyi and Kok,

2020). We find that our parameterization reproduces the abundance of super coarse dust close to dust source regions. However, the model still substantially underestimates super coarse dust in dust outflow regions, presumably due to errors in numerical diffusion or missing processes during dust transport and deposition. We find that the net effect of these model errors and missing processes is to underestimate the super coarse dust lifetime by an order of magnitude, which is equivalent to decreasing the effective dust aerosol density in our model (CESM) to an order of magnitude less than its physical value of ~2,500 kg/m^3. Therefore, the underestimation of super coarse atmospheric dust by models is in part due to the underestimation of the emission of super coarse dust, which can be resolved by implementing the parameterization presented here, and in part due to errors in deposition processes, which requires further work to resolve but can be ameliorated by articially reducing the dust density.

Acknowledgments

J. Meng and J. F. Kok acknowledge the financial support by the National Science Foundation (NSF) (1856389) and the Army Research Office (cooperative agreement number

W911NF-20-2-0150). Y. Huang acknowledges the financial support by the Columbia University Earth Institute Postdoctoral Research Fellowship and the National Aeronautics and Space Administration (NASA) grant 80NSSC19K1346, awarded under the Future Investigators in NASA Earth and Space Science and Technology (FINESST) program. We acknowledge high-performance computing support from Cheyenne (https://doi.org/10.5065/D6RX99HX, last access: 1 Sept. 2021) provided by NCAR's Computational and Information Systems Laboratory, sponsored by the National Science Foundation. The MERRA-2 data used in this study have been provided by the Global Modeling and Assimilation Office (GMAO) at NASA Goddard Space Flight Center. The views and conclusions contained in this document are those of the authors and should not be interpreted as representing the official policies, either expressed or implied, of the Army Research Laboratory or the US Government.

Open Research

A supplemental file containing the dust mass fractions for dust bins covering the 0.1 to 100 µm size range is available in this Zenodo repository (https://doi.org/10.5281/zenodo.5762577) with a DOI of 10.5281/zenodo.5762577. The modified CESM source codes are available in this GitHub repository (https://doi.org/10.5281/zenodo.5762587) with a DOI of 10.5281/zenodo.5762587. The data on which Tables S1 and S2 are based are available in Chandler et al. (2004), Li et al. (2014), Mei et al. (2004), Swet and Katra (2016), Liu et al. (1998), Su et al. (2007), Klost et al. (2017), Shao et al. (2011), Ryder, Highwood, Rosenberg, et al. (2013) and Ryder et al (2015).

References

https://doi.org/10.1175/1520-0450(1972)011%3c0977:MOASDA%3e2.0.CO;2

https://doi.org/10.1029/JC079i027p04068

https://doi.org/10.1029/2019JD031185

https://doi.org/10.5194/acp-9-3881-2009

Adebiyi, A. A., & Kok, J. F. (2020). Climate models miss most of the coarse dust in the atmosphere. *Science Advances*, *6*(15), eaaz9507. https://doi.org/10.1126/sciadv.aaz9507Adebiyi, A. A., Kok, J. F., Wang, Y., Ito, A., Ridley, D. A., Nabat, P., & Zhao, C. (2020). Dust Constraints from joint Observational-Modelling-experiMental analysis (DustCOMM): comparison with measurements and model simulations. *Atmospheric Chemistry and Physics*, *20*(2), 829–863. https://doi.org/10.5194/acp-20-829-2020Albani, S., Mahowald, N. M., Perry, A. T., Scanza, R. A., Zender, C. S., Heavens, N. G., et al. (2014). Improved dust representation in the Community Atmosphere Model. *Journal of Advances in Modeling Earth Systems*, *6*(3), 541–570. https://doi.org/10.1002/2013MS000279Ansmann, A., Rittmeister, F., Engelmann, R., Basart, S., Jorba, O., Spyrou, C., et al. (2017). Profiling of Saharan dust from the Caribbean to western Africa – Part 2: Shipborne lidar measurements versus forecasts. *Atmospheric Chemistry and Physics*, *17*(24), 14987–15006. https://doi.org/10.5194/acp-17-14987-2017Braunack, M. V., Hewitt, J. S., & Dexter, A. R. (1979). Brittle Fracture of Soil Aggregates and the Compaction of Aggregate Beds. *Journal of Soil Science*, *30*(4), 653–667. https://doi.org/10.1111/j.1365-2389.1979.tb01015.xButler, H., Leys, J., Strong, C., & McTainsh, G. (2013). *Caring for our country: wind erosion extent and severity maps for Australia, final report*. Retrieved from https://1library.net/document/oz12g63y-caring-country-erosion-extent-severity-australia-final-report.htmlChatenet, B., Marticorena, B., Gomes, L., & Bergametti, G. (1996). Assessing the microped size distributions of desert soils erodible by wind. *Sedimentology*, *43*(5), 901–911. https://doi.org/10.1111/j.1365-3091.1996.tb01509.xChen, Q., Yin, Y., Jiang, H., Chu, Z., Xue, L., Shi, R., et al. (2019). The Roles of Mineral Dust as Cloud Condensation Nuclei and Ice Nuclei During the Evolution of a Hail Storm. *Journal of Geophysical Research: Atmospheres*, *124*(24), 14262–14284. https://doi.org/10.1029/2019JD031403Cowie, S. M., Marsham, J. H., & Knippertz, P. (2015). The importance of rare, high-wind events for dust uplift in northern Africa. *Geophysical Research Letters*, *42*(19), 8208–8215. https://doi.org/10.1002/2015GL065819Di Biagio, C., Balkanski, Y., Albani, S., Boucher, O., & Formenti, P. (2020). Direct Radiative Effect by Mineral Dust Aerosols Constrained by New Microphysical and Spectral Optical Data. *Geophysical Research Letters*, *47*(2), e2019GL086186. https://doi.org/10.1029/2019GL086186van der Does, M., Knippertz, P., Zschenderlein, P., Giles Harrison, R., & Stuut, J.-B. W. (2018). The mysterious long-range transport of giant mineral dust particles. *Science Advances*, *4*(12), eaau2768. https://doi.org/10.1126/sciadv.aau2768Fratini, G., Ciccioli, P., Febo, A., Forgione, A., & Valentini, R. (2007). Size-segregated fluxes of mineral dust from a desert area of northern China by

eddy covariance. Atmospheric Chemistry and Physics, 7(11), 2133–2168. https://doi.org/10.5194/acpd-7-2133-2007Gasteiger, J., Groß, S., Sauer, D., Haarig, M., Ansmann, A., & Weinzierl, B. (2017). Particle settling and vertical mixing in the Saharan Air Layer as seen from an integrated model, lidar, and in situ perspective. *Atmospheric Chemistry and Physics*, *17*(1), 297–311. https://doi.org/10.5194/acp-17-297-2017Gillette, D. A. (1974). On the production of soil wind erosion aerosols having the potential for long range transport. Journal de Recherches Atmospheriques, 8, 734–744.Gillette, D. A., Blifford, I. H., Jr., & Fenster, C. R. (1972). Measurements of aerosol size distributions and vertical fluxes of aerosols on land subject to wind erosion. Journal of Applied Meteorology, 11(6), 977–987. Gillette, D. A., Blifford, I. H., Jr., & Fryrear, D. W. (1974). The influence of wind velocity on the size distributions of aerosols generated by the wind erosion of soils. Journal of Geophysical Research, 79(27), 4068–4075. Ginoux, P. (2003). Effects of nonsphericity on mineral dust modeling. *Journal of Geophysical Research: Atmospheres*, *108*(D2). https://doi.org/10.1029/2002JD002516Guieu, C., Azhar, M. A., Aumont, O., Mahowald, N., Levy, M., Ethé, C., & Lachkar, Z. (2019). Major Impact of Dust Deposition on the Productivity of the Arabian Sea. *Geophysical Research Letters*, *46*(12), 6736–6744. https://doi.org/10.1029/2019GL082770Heisel, M., Chen, B., Kok, J. F., & Chamecki, M. (2021). Gentle Topography Increases Vertical Transport of Coarse Dust by Orders of Magnitude. *Journal of Geophysical Research: Atmospheres*, *126*(14), e2021JD034564. https://doi.org/10.1029/2021JD034564Herrmann, H. J., & Roux, S. (2014). *Statistical Models for the Fracture of Disordered Media*. Elsevier.Huang, Y., Kok, J. F., Martin, R. L., Swet, N., Katra, I., Gill, T. E., et al. (2019). Fine dust emissions from active sands at coastal Oceano Dunes, California. *Atmospheric Chemistry and Physics*, *19*(5), 2947–2964. https://doi.org/10.5194/acp-19-2947-2019Huang, Y., Kok, J. F., Kandler, K., Lindqvist, H., Nousiainen, T., Sakai, T., et al. (2020). Climate Models and Remote Sensing Retrievals Neglect Substantial Desert Dust Asphericity. *Geophysical Research Letters*, *47*(6), e2019GL086592. https://doi.org/10.1029/2019GL086592Huang, Y., Adebiyi, A. A., Formenti, P., & Kok, J. F. (2021). Linking the Different Diameter Types of Aspherical Desert Dust Indicates That Models Underestimate Coarse Dust Emission. *Geophysical Research Letters*, *48*(6), e2020GL092054. https://doi.org/10.1029/2020GL092054Hurrell, J. W., Holland, M. M., Gent, P. R., Ghan, S., Kay, J. E., Kushner, P. J., et al. (2013). The Community Earth System Model: A Framework for Collaborative Research. *Bulletin of the American Meteorological Society*, *94*(9), 1339–1360. https://doi.org/10.1175/BAMS-D-12-00121.1Ito, A., Kok, J. F., Feng, Y., & Penner, J. E. (2012). Does a theoretical estimation of the dust size distribution at emission suggest more bioavailable iron deposition? *Geophysical Research Letters*, *39*(5). https://doi.org/10.1029/2011GL050455Jickells, T. D., An, Z. S., Andersen, K. K., Baker, A. R., Bergametti, G., Brooks, N., et al. (2005). Global Iron Connections Between Desert Dust, Ocean Biogeochemistry, and Climate. *Science*, *308*(5718), 67–71. https://doi.org/10.1126/science.1105959Khalfallah, B., Bouet, C., Labiadh, M. T., Alfaro, S. C., Bergametti, G., Marticorena, B.,

et al. (2020). Influence of atmospheric stability on the size distribution of the vertical dust flux measured in eroding conditions over a flat bare sandy field. Journal of Geophysical Research: Atmospheres, 125(4), 1–20. Klose, M., & Shao, Y. (2012). Stochastic parameterization of dust emission and application to convective atmospheric conditions. *Atmospheric Chemistry and Physics*, *12*(16), 7309–7320. https://doi.org/10.5194/acp-12-7309-2012Klose, Martina, Gill, T. E., Webb, N. P., & Van Zee, J. W. (2017). Field sampling of loose erodible material: A new system to consider the full particle-size spectrum. *Aeolian Research*, *28*, 83–90. https://doi.org/10.1016/j.aeolia.2017.08.003Kok, J. F. (2011a). A scaling theory for the size distribution of emitted dust aerosols suggests climate models underestimate the size of the global dust cycle. *Proceedings of the National Academy of Sciences*, *108*(3), 1016–1021. https://doi.org/10.1073/pnas.1014798108Kok, J. F. (2011b). Does the size distribution of mineral dust aerosols depend on the wind speed at emission? *Atmospheric Chemistry and Physics*, *11*(19), 10149–10156. https://doi.org/10.5194/acp-11-10149-2011Kok, J. F., Mahowald, N. M., Fratini, G., Gillies, J. A., Ishizuka, M., Leys, J. F., et al. (2014). An improved dust emission model – Part 1: Model description and comparison against measurements. *Atmospheric Chemistry and Physics*, *14*(23), 13023–13041. https://doi.org/10.5194/acp-14-13023-2014Kok, J. F., Albani, S., Mahowald, N. M., & Ward, D. S. (2014). An improved dust emission model – Part 2: Evaluation in the Community Earth System Model, with implications for the use of dust source functions. *Atmospheric Chemistry and Physics*, *14*(23), 13043–13061. https://doi.org/10.5194/acp-14-13043-2014Kok, J. F., Ridley, D. A., Zhou, Q., Miller, R. L., Zhao, C., Heald, C. L., et al. (2017). Smaller desert dust cooling effect estimated from analysis of dust size and abundance. *Nature Geoscience*, *10*(4), 274–278. https://doi.org/10.1038/ngeo2912Kok, Jasper F., Adebiyi, A. A., Albani, S., Balkanski, Y., Checa-Garcia, R., Chin, M., et al. (2021). Improved representation of the global dust cycle using observational constraints on dust properties and abundance. *Atmospheric Chemistry and Physics*, *21*(10), 8127–8167. https://doi.org/10.5194/acp-21-8127-2021Kosmopoulos, P. G., Kazadzis, S., Taylor, M., Athanasopoulou, E., Speyer, O., Raptis, P. I., et al. (2017). Dust impact on surface solar irradiance assessed with model simulations, satellite observations and ground-based measurements. *Atmospheric Measurement Techniques*, *10*(7), 2435–2453. https://doi.org/10.5194/amt-10-2435-2017Laurent, B., Marticorena, B., Bergametti, G., & Mei, F. (2006). Modeling mineral dust emissions from Chinese and Mongolian deserts. *Global and Planetary Change*, *52*(1), 121–141. https://doi.org/10.1016/j.gloplacha.2006.02.012Mahowald, N., Albani, S., Kok, J. F., Engelstaeder, S., Scanza, R., Ward, D. S., & Flanner, M. G. (2014). The size distribution of desert dust aerosols and its impact on the Earth system. *Aeolian Research*, *15*, 53–71. https://doi.org/10.1016/j.aeolia.2013.09.002Meng, J., Martin, R. V., Ginoux, P., Hammer, M., Sulprizio, M. P., Ridley, D. A., & van Donkelaar, A. (2021). Grid-independent high-resolution dust emissions (v1.0) for chemical transport models: application to GEOS-Chem (12.5.0). *Geoscientific Model Development*, *14*(7), 4249–4260. https://doi.org/10.5194/gmd-

14-4249-2021Neale, R. B., Richter, J. H., Conley, A. J., Park, S., Lauritzen, P. H., Gettelman, A., et al. (2010). *Description of the NCAR Community Atmosphere Model*.Oddershede, L., Dimon, P., & Bohr, J. (1993). Self-organized criticality in fragmenting. *Physical Review Letters*, *71*(19), 3107–3110. https://doi.org/10.1103/PhysRevLett.71.3107Perfect, E., & Kay, B. D. (1995). Brittle Fracture of Fractal Cubic Aggregates. *Soil Science Society of America Journal*, *59*(4), 969–974. https://doi.org/10.2136/sssaj1995.03615995005900040002xRastigejev, Y., Park, R., Brenner, M. P., & Jacob, D. J. (2010). Resolving intercontinental pollution plumes in global models of atmospheric transport. *Journal of Geophysical Research: Atmospheres*, *115*(D2). https://doi.org/10.1029/2009JD012568Renard, J.-B., Dulac, F., Durand, P., Bourgeois, Q., Denjean, C., Vignelles, D., et al. (2018). In situ measurements of desert dust particles above the western Mediterranean Sea with the balloon-borne Light Optical Aerosol Counter/sizer (LOAC) during the ChArMEx campaign of summer 2013. *Atmospheric Chemistry and Physics*, *18*(5), 3677–3699. https://doi.org/10.5194/acp-18-3677-2018Roberts, A. J., Marsham, J. H., Knippertz, P., Parker, D. J., Bart, M., Garcia-Carreras, L., et al. (2017). New Saharan wind observations reveal substantial biases in analysed dust-generating winds. *Atmospheric Science Letters*, *18*(9), 366–372. https://doi.org/10.1002/asl.765Rosenberg, P. D., Parker, D. J., Ryder, C. L., Marsham, J. H., Garcia-Carreras, L., Dorsey, J. R., et al. (2014). Quantifying particle size and turbulent scale dependence of dust flux in the Sahara using aircraft measurements. *Journal of Geophysical Research: Atmospheres*, *119*(12), 7577–7598. https://doi.org/10.1002/2013JD021255Ryder, C. L., Highwood, E. J., Lai, T. M., Sodemann, H., & Marsham, J. H. (2013). Impact of atmospheric transport on the evolution of microphysical and optical properties of Saharan dust. *Geophysical Research Letters*, *40*(10), 2433–2438. https://doi.org/10.1002/grl.50482Ryder, C. L., Highwood, E. J., Rosenberg, P. D., Trembath, J., Brooke, J. K., Bart, M., et al. (2013). Optical properties of Saharan dust aerosol and contribution from the coarse mode as measured during the Fennec 2011 aircraft campaign. *Atmospheric Chemistry and Physics*, *13*(1), 303–325. https://doi.org/10.5194/acp-13-303-2013Ryder, C. L., McQuaid, J. B., Flamant, C., Rosenberg, P. D., Washington, R., Brindley, H. E., et al. (2015). Advances in understanding mineral dust and boundary layer processes over the Sahara from Fennec aircraft observations. *Atmospheric Chemistry and Physics*, *15*(14), 8479–8520. https://doi.org/10.5194/acp-15-8479-2015Ryder, C. L., Marenco, F., Brooke, J. K., Estelles, V., Cotton, R., Formenti, P., et al. (2018). Coarse-mode mineral dust size distributions, composition and optical properties from AER-D aircraft measurements over the tropical eastern Atlantic. *Atmospheric Chemistry and Physics*, *18*(23), 17225–17257. https://doi.org/10.5194/acp-18-17225-2018Ryder, C. L., Highwood, E. J., Walser, A., Seibert, P., Philipp, A., & Weinzierl, B. (2019). Coarse and giant particles are ubiquitous in Saharan dust export regions and are radiatively significant over the Sahara. *Atmospheric Chemistry and Physics*, *19*(24), 15353–15376. https://doi.org/10.5194/acp-19-15353-2019Shao, Y. (2008). *Physics and Modelling of Wind Erosion* (2nd ed.). Springer Netherlands. https://doi.org/10.1007/978-1-4020-8895-7Shao, Y., Ishizuka,

M., Mikami, M., & Leys, J. F. (2011). Parameterization of size-resolved dust emission and validation with measurements. *Journal of Geophysical Research: Atmospheres*, *116*(D8). https://doi.org/10.1029/2010JD014527Shao, Y., Zhang, J., Ishizuka, M., Mikami, M., Leys, J., & Huang, N. (2020). Dependency of particle size distribution at dust emission on friction velocity and atmospheric boundary-layer stability. *Atmospheric Chemistry and Physics*, *20*(21), 12939–12953. https://doi.org/10.5194/acp-20-12939-2020Sow, M., Alfaro, S. C., Rajot, J. L., & Marticorena, B. (2009). Size resolved dust emission fluxes measured in Niger during 3 dust storms of the AMMA experiment. Atmospheric Chemistry and Physics, 9(12), 3881–3891. Ulanowski, Z., Bailey, J., Lucas, P. W., Hough, J. H., & Hirst, E. (2007). Alignment of atmospheric mineral dust due to electric field. *Atmospheric Chemistry and Physics*, *7*(24), 6161–6173. https://doi.org/10.5194/acp-7-6161-2007Varga, G., Dagsson-Walhauserová, P., Gresina, F., & Helgadottir, A. (2021). Saharan dust and giant quartz particle transport towards Iceland. *Scientific Reports*, *11*(1), 11891. https://doi.org/10.1038/s41598-021-91481-zWagner, F., Bortoli, D., Pereira, S., Costa, M. Jo., Silva, A. M., Weinzierl, B., et al. (2009). Properties of dust aerosol particles transported to Portugal from the Sahara desert. *Tellus B: Chemical and Physical Meteorology*, *61*(1), 297–306. https://doi.org/10.1111/j.1600-0889.2008.00393.xvon der Weiden, S.-L., Drewnick, F., & Borrmann, S. (2009). Particle Loss Calculator – a new software tool for the assessment of the performance of aerosol inlet systems. *Atmospheric Measurement Techniques*, *2*(2), 479–494. https://doi.org/10.5194/amt-2-479-2009Weinzierl, B., Ansmann, A., Prospero, J. M., Althausen, D., Benker, N., Chouza, F., et al. (2017). The Saharan Aerosol Long-Range Transport and Aerosol–Cloud-Interaction Experiment: Overview and Selected Highlights. *Bulletin of the American Meteorological Society*, *98*(7), 1427–1451. https://doi.org/10.1175/BAMS-D-15-00142.1Wu, M., Liu, X., Yu, H., Wang, H., Shi, Y., Yang, K., et al. (2020). Understanding processes that control dust spatial distributions with global climate models and satellite observations. *Atmospheric Chemistry and Physics*, *20*(22), 13835–13855. https://doi.org/10.5194/acp-20-13835-2020Zender, C. S., Bian, H., & Newman, D. (2003). Mineral Dust Entrainment and Deposition (DEAD) model: Description and 1990s dust climatology. *Journal of Geophysical Research: Atmospheres*, *108*(D14). https://doi.org/10.1029/2002JD002775Zhang, L., Kok, J. F., Henze, D. K., Li, Q., & Zhao, C. (2013). Improving simulations of fine dust surface concentrations over the western United States by optimizing the particle size distribution. *Geophysical Research Letters*, *40*(12), 3270–3275. https://doi.org/10.1002/grl.50591

References From the Supporting Information

Åström, J. A. (2006). Statistical models of brittle fragmentation. *Advances in Physics*, *55*(3–4), 247–278. https://doi.org/10.1080/00018730600731907

https://doi.org/10.1063/1.1736017

https://doi.org/10.1002/essoar.10506234.1

Chandler, D. G., Saxton, K. E., & Busacca, A. J. (2004). Predicting Wind Erodibility of Loessial Soils in the Pacific Northwest by Particle Sizing. *Arid Land Research and Management*, *19*(1), 13–27. https://doi.org/10.1080/15324980590887074Chatenet, B., Marticorena, B., Gomes, L., & Bergametti, G. (1996). Assessing the microped size distributions of desert soils erodible by wind. *Sedimentology*, *43*(5), 901–911. https://doi.org/10.1111/j.1365-3091.1996.tb01509.xFormenti, P., Schütz, L., Balkanski, Y., Desboeufs, K., Ebert, M., Kandler, K., et al. (2011). Recent progress in understanding physical and chemical properties of African and Asian mineral dust. *Atmospheric Chemistry and Physics*, *11*(16), 8231–8256. https://doi.org/10.5194/acp-11-8231-2011Gelaro, R., McCarty, W., Suárez, M. J., Todling, R., Molod, A., Takacs, L., et al. (2017). The Modern-Era Retrospective Analysis for Research and Applications, Version 2 (MERRA-2). *Journal of Climate*, *30*(14), 5419–5454. https://doi.org/10.1175/JCLI-D-16-0758.1Gilvarry, J. J., & Bergstrom, B. H. (1961). Fracture of Brittle Solids. II. Distribution Function for Fragment Size in Single Fracture (Experimental). *Journal of Applied Physics*, *32*(3), 400–410. Huang, Y., Adebiyi, A. A., Formenti, P., & Kok, J. F. (2021). Linking the Different Diameter Types of Aspherical Desert Dust Indicates That Models Underestimate Coarse Dust Emission. *Geophysical Research Letters*, *48*(6), e2020GL092054. https://doi.org/10.1029/2020GL092054Hurrell, J. W., Holland, M. M., Gent, P. R., Ghan, S., Kay, J. E., Kushner, P. J., et al. (2013). The Community Earth System Model: A Framework for Collaborative Research. *Bulletin of the American Meteorological Society*, *94*(9), 1339–1360. https://doi.org/10.1175/BAMS-D-12-00121.ISO. (2009). Determination of particle size distribution: single particle light interaction methods, Part 1: Light scattering aerosol spectrometer. ISO 21501-1 Klose, M., Gill, T. E., Webb, N. P., & Van Zee, J. W. (2017). Field sampling of loose erodible material: A new system to consider the full particle-size spectrum. *Aeolian Research*, *28*, 83–90. https://doi.org/10.1016/j.aeolia.2017.08.003Kok, J. F. (2011). A scaling theory for the size distribution of emitted dust aerosols suggests climate models underestimate the size of the global dust cycle. *Proceedings of the National Academy of Sciences*, *108*(3), 1016–1021. https://doi.org/10.1073/pnas.1014798108Kok, J. F., Mahowald, N. M., Fratini, G., Gillies, J. A., Ishizuka, M., Leys, J. F., et al. (2014). An improved dust emission model – Part 1: Model description and comparison against measurements. *Atmospheric Chemistry and Physics*, *14*(23), 13023–13041. https://doi.org/10.5194/acp-14-13023-2014Kok, J. F., Albani, S., Mahowald, N. M., & Ward, D. S. (2014). An improved dust emission model – Part 2: Evaluation in the Community Earth System Model, with implications for the use of dust source functions. *Atmospheric Chemistry and Physics*, *14*(23), 13043–13061. https://doi.org/10.5194/acp-14-13043-2014Lawrence, D. M., Oleson, K. W., Flanner, M. G., Thornton, P. E., Swenson, S. C., Lawrence, P. J., et al. (2011). Parameterization improvements and functional and structural advances in Version 4 of the Community Land Model. *Journal of Advances in Modeling Earth Systems*, *3*(1). https://doi.org/10.1029/2011MS00045Leung,

D. M., Kok, J., Li, L., Mahowald, N., MENUT, L., Prigent, C., et al. (2020). Improving the parameterization of dust emission threshold in the Community Earth System Model (CESM). In *Earth and Space Science Open Archive*. Earth and Space Science Open Archive. Li, X., Feng, G., Sharratt, B. S., Zheng, Z., Pi, H., & Gao, F. (2014). Soil Wind Erodibility Based on Dry Aggregate-Size Distribution in the Tarim Basin. *Soil Science Society of America Journal*, *78*(6), 2009–2016. https://doi.org/10.2136/sssaj2014.06.0235Liu, L., Wang, J., Li, X., Liu, Y., Ta, W., & Peng, H. (1998). Determination of erodible particles on cultivated soils by wind tunnel simulation. *Chinese Science Bulletin*, *43*(19), 1646–1651. https://doi.org/10.1007/BF02883411Mahowald, N. M., Muhs, D. R., Levis, S., Rasch, P. J., Yoshioka, M., Zender, C. S., & Luo, C. (2006). Change in atmospheric mineral aerosols in response to climate: Last glacial period, preindustrial, modern, and doubled carbon dioxide climates. *Journal of Geophysical Research: Atmospheres*, *111*(D10). https://doi.org/10.1029/2005JD006653Mei, F., Zhang, X., Lu, H., Shen, Z., & Wang, Y. (2004). Characterization of MASDs of surface soils in north China and its influence on estimating dust emission. *Chinese Science Bulletin*, *49*(20), 2169–2176. https://doi.org/10.1007/BF03185784Meng, Z., Yang, P., Kattawar, G. W., Bi, L., Liou, K. N., & Laszlo, I. (2010). Single-scattering properties of tri-axial ellipsoidal mineral dust aerosols: A database for application to radiative transfer calculations. *Journal of Aerosol Science*, *41*(5), 501–512. https://doi.org/10.1016/j.jaerosci.2010.02.008Neale, R. B., Richter, J. H., Conley, A. J., Park, S., Lauritzen, P. H., Gettelman, A., et al. (2010). *Description of the NCAR Community Atmosphere Model*.Rosenberg, P. D., Dean, A. R., Williams, P. I., Dorsey, J. R., Minikin, A., Pickering, M. A., & Petzold, A. (2012). Particle sizing calibration with refractive index correction for light scattering optical particle counters and impacts upon PCASP and CDP data collected during the Fennec campaign. *Atmospheric Measurement Techniques*, *5*(5), 1147–1163. https://doi.org/10.5194/amt-5-1147-2012Ryder, C. L., Highwood, E. J., Lai, T. M., Sodemann, H., & Marsham, J. H. (2013). Impact of atmospheric transport on the evolution of microphysical and optical properties of Saharan dust. *Geophysical Research Letters*, *40*(10), 2433–2438. https://doi.org/10.1002/grl.50482Ryder, C. L., Highwood, E. J., Rosenberg, P. D., Trembath, J., Brooke, J. K., Bart, M., et al. (2013). Optical properties of Saharan dust aerosol and contribution from the coarse mode as measured during the Fennec 2011 aircraft campaign. *Atmospheric Chemistry and Physics*, *13*(1), 303–325. https://doi.org/10.5194/acp-13-303-2013Ryder, C. L., McQuaid, J. B., Flamant, C., Rosenberg, P. D., Washington, R., Brindley, H. E., et al. (2015). Advances in understanding mineral dust and boundary layer processes over the Sahara from Fennec aircraft observations. *Atmospheric Chemistry and Physics*, *15*(14), 8479–8520. https://doi.org/10.5194/acp-15-8479-2015Shao, Y., Ishizuka, M., Mikami, M., & Leys, J. F. (2011). Parameterization of size-resolved dust emission and validation with measurements. *Journal of Geophysical Research: Atmospheres*, *116*(D8). https://doi.org/10.1029/2010JD014527Su, Y., Wang, F., Zhang, Z., & Du, M. (2007). Soil Properties and Characteristics of Soil

Aggregate in Marginal Farmlands of Oasis in the Middle of Hexi Corridor Region, Northwest China. *Agricultural Sciences in China*, *6*(6), 706–714. https://doi.org/10.1016/S1671-2927(07)60103-5Swet, N., & Katra, I. (2016). Reduction in soil aggregation in response to dust emission processes. *Geomorphology*, *268*, 177–183. https://doi.org/10.1016/j.geomorph.2016.06.002Wagner, F., Bortoli, D., Pereira, S., Costa, M. Jo., Silva, A. M., Weinzierl, B., et al. (2009). Properties of dust aerosol particles transported to Portugal from the Sahara desert. *Tellus B: Chemical and Physical Meteorology*, *61*(1), 297–306. https://doi.org/10.1111/j.1600-0889.2008.00393.xWeinzierl, B., Petzold, A., Esselborn, M., Wirth, M., Rasp, K., Kandler, K., et al. (2009). Airborne measurements of dust layer properties, particle size distribution and mixing state of Saharan dust during SAMUM 2006. *Tellus B: Chemical and Physical Meteorology*, *61*(1), 96–117. https://doi.org/10.1111/j.1600-0889.2008.00392.xWeinzierl, B., Ansmann, A., Prospero, J. M., Althausen, D., Benker, N., Chouza, F., et al. (2017). The Saharan Aerosol Long-Range Transport and Aerosol–Cloud-Interaction Experiment: Overview and Selected Highlights. *Bulletin of the American Meteorological Society*, *98*(7), 1427–1451. https://doi.org/10.1175/BAMS-D-15-00142.1Zender, C. S., Bian, H., & Newman, D. (2003). Mineral Dust Entrainment and Deposition (DEAD) model: Description and 1990s dust climatology. *Journal of Geophysical Research: Atmospheres*, *108*(D14). https://doi.org/10.1029/2002JD002775 Fratini, G., Ciccioli, P., Febo, A., Forgione, A., & Valentini, R. (2007). Size-segregated fluxes of mineral dust from a desert area of northern China by eddy covariance. Atmospheric Chemistry and Physics, 7(11), 2133–2168. https://doi.org/10.5194/acpd-7-2133-2007

Gillette, D. A. (1974). On the production of soil wind erosion aerosols having the potential for long range transport. Journal de Recherches Atmospheriques, 8, 734–744.

Gillette, D. A., Blifford, I. H., Jr., & Fenster, C. R. (1972). Measurements of aerosol size distributions and vertical fluxes of aerosols on land subject to wind erosion. Journal of Applied Meteorology, 11(6), 977–987. https://doi.org/10.1175/1520-0450(1972)011%3c0977:MOASDA%3e2.0.CO;2

Gillette, D. A., Blifford, I. H., Jr., & Fryrear, D. W. (1974). The influence of wind velocity on the size distributions of aerosols generated by the wind erosion of soils. Journal of Geophysical Research, 79(27), 4068–4075. https://doi.org/10.1029/JC079i027p04068

Khalfallah, B., Bouet, C., Labiadh, M. T., Alfaro, S. C., Bergametti, G., Marticorena, B., et al. (2020). Influence of atmospheric stability on the size distribution of the vertical dust flux measured in eroding conditions over a flat bare sandy field. Journal of Geophysical Research: Atmospheres, 125(4), 1–20. https://doi.org/10.1029/2019JD031185

Rosenberg, P. D., Parker, D. J., Ryder, C. L., Marsham, J. H., Garcia-Carreras, L., Dorsey, J. R., et al. (2014). Quantifying particle size and turbulent scale

dependence of dust flux in the Sahara using aircraft measurements. Journal of Geophysical Research: Atmospheres, 119(12), 7577–7598. https://doi.org/10.1002/2013JD021255

Sow, M., Alfaro, S. C., Rajot, J. L., & Marticorena, B. (2009). Size resolved dust emission fluxes measured in Niger during 3 dust storms of the AMMA experiment. Atmospheric Chemistry and Physics, 9(12), 3881–3891. https://doi.org/10.5194/acp-9-3881-2009